Osmotin Is a Homolog of Mammalian Adiponectin and Controls Apoptosis in Yeast through a Homolog of Mammalian Adiponectin Receptor

Meena L. Narasimhan,[1,6] María A. Coca, [1,6] Jingbo Jin,[1]
Toshimasa Yamauchi,[2] Yusuke Ito,[2]
Takashi Kadowaki,[2] Kyeong Kyu Kim,[3]
José M. Pardo,[4] Barbara Damsz,[1]
Paul M. Hasegawa,[1] Dae-Jin Yun,[5,*]
and Ray A. Bressan[1]
[1]Center for Plant Environmental Stress Physiology
Purdue University
625 Agriculture Mall Drive
West Lafayette, Indiana 47907
[2]Department of Metabolic Disease
Graduate School of Medicine
University of Tokyo
7-3-1 Hongo, Bunkyo-ku, Tokyo
Japan
[3]Department of Molecular Cell Biology
Center for Molecular Medicine
SBRI
Sungkyunkwan University School of Medicine
Suwon
Korea
[4]Instituto de Recursos Naturales y Agrobiología
C.S.I.C.
Apartado 1052
41080 Sevilla
Spain
[5]Environmental Biotechnology National Core
   Research Center and
Division of Applied Life Science (BK21 Program)
Graduate School of Gyeongsang National University
Jinju 660-701
Korea

Summary

The antifungal activity of the PR-5 family of plant defense proteins has been suspected to involve specific plasma membrane component(s) of the fungal target. Osmotin is a tobacco PR-5 family protein that induces apoptosis in the yeast *Saccharomyces cerevisiae.* We show here that the protein encoded by *ORE20/PHO36 (YOL002c)*, a seven transmembrane domain receptor-like polypeptide that regulates lipid and phosphate metabolism, is an osmotin binding plasma membrane protein that is required for full sensitivity to osmotin. *PHO36* functions upstream of *RAS2* in the osmotin-induced apoptotic pathway. The mammalian homolog of PHO36 is a receptor for the hormone adiponectin and regulates cellular lipid and sugar metabolism. Osmotin and adiponectin, the corresponding "receptor" binding proteins, do not share sequence similarity. However, the β barrel domain of both proteins can be overlapped, and osmotin, like adiponectin, activates AMP kinase in C2C12 myocytes via adiponectin receptors.

*Correspondence: djyun@gsnu.ac.kr
[6]These authors contributed equally to this work.

Introduction

Among families of antimicrobial proteins associated with plant defense are the *p*athogenesis-*r*elated proteins of family *5* (PR-5) that are structurally related to the sweet-tasting protein thaumatin (Veronese et al., 2003). Osmotin is an antifungal tobacco PR-5 protein. It induces programmed cell death in *Saccharomyces cerevisiae* by signaling suppression of cellular stress responses via RAS2/cAMP (Narasimhan et al., 2001).

Most of the PR proteins, including osmotin, have specific wide-spectrum antifungal activities, suggesting that target recognition may be determined by their interaction with pathogen cell surface components. Specific fungal cell wall components enhance or suppress osmotin antifungal activity (Narasimhan et al., 2003; Veronese et al., 2003). In *S. cerevisiae*, the PIR family of cell wall glycoproteins are osmotin resistance determinants (Yun et al., 1997), whereas phosphomannans of cell wall glycoproteins have been shown to increase osmotin toxicity, probably by serving as docking structures to facilitate osmotin diffusion across the cell wall (Ibeas et al., 2000). Genetic analyses have revealed that SSD1, a protein that affects cell wall morphogenesis and deposition of PIR proteins, is a critical determinant of resistance to osmotin (Ibeas et al., 2001). Unidentified changes in the yeast cell wall that enhance toxicity are induced by osmotin via activation of a mitogen-activated protein kinase cascade (Yun et al., 1998).

Specific interactions at the plasma membrane are also required for osmotin antifungal activity, because yeast spheroplasts that are susceptible to tobacco osmotin can be resistant to PR-5 proteins from other plant species (Yun et al., 1997). We report here the isolation of a plasma membrane determinant of osmotin sensitivity that was identified by its ability to confer an osmotin supersensitive phenotype to yeast cells upon gene overexpression. The gene, *ORE20/PHO36*, encodes a seven transmembrane domain receptor-like protein, homologous to mammalian adiponectin receptors, and is involved in yeast lipid and phosphate metabolism (Karpichev et al., 2002; Yamauchi et al., 2003a). Adiponectin is an antidiabetic and antiatherosclerotic protein hormone in mammals that conditions sensing of energy status, fatty acid oxidation, and glucose transport upon interaction with adiponectin receptors (Diez and Iglesias, 2003; Yamauchi et al., 2003a, 2003b). The nature of the PHO36 ligand is unknown. We report that ORE20/PHO36 specifically binds osmotin at the plasma membrane and controls osmotin-induced cell death via a *RAS2* signaling pathway. We also show that osmotin can induce AMP kinase phosphorylation in mammalian C2C12 myocytes via adiponectin receptors.

Results

PHO36 Mediates Sensitivity to Osmotin
Genes that conferred an osmotin supersensitive phenotype to the yeast strain BWG7a were isolated using a
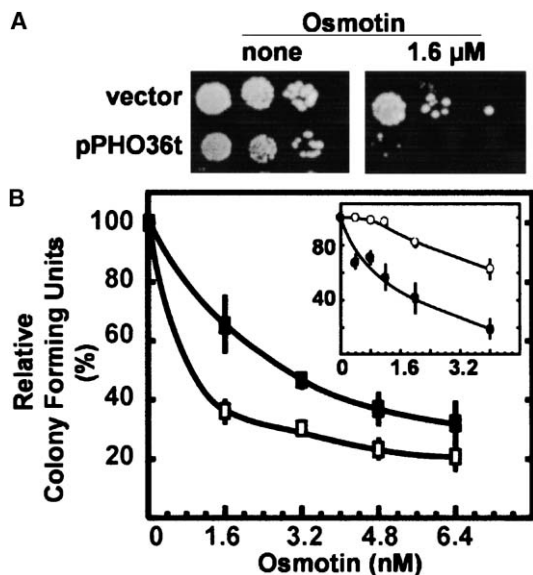
A

B

Figure 1. *PHO36* Mediates Sensitivity to Osmotin in Yeast

(A) Aliquots (2.5 μl) of 10-fold serial dilutions of log phase cultures (A_{600nm} 0.4) of the yeast strain BWG7a transformed with the centromeric plasmid pRS316 without (vector) or with *PHO36t* insert (pPHO36t) were spotted on selective SC-galactose media without (none) or with osmotin supplement (1.6 μM) and allowed to grow for 3 days at 28°C.

(B) Spheroplasts (10^6 ml^{-1}) derived from the wild-type strain BWG7a ($\square$) or the isogenic $\Delta pho36$ mutant ($\blacksquare$) were diluted and plated in YPD agar containing 0.8 M sorbitol and the indicated concentrations of osmotin. Viable spheroplasts were counted after 3 days incubation at 28°C. Viable counts are normalized to the value without added osmotin. Values are the average of three different experiments ±SE. (Inset) Results of a similar experiment with spheroplasts of BWG7a strain carrying the plasmid pRS316 without ($\bigcirc$) or with *PHO36t* insert (pPHO36t; $\bullet$), performed in selective SC-galactose media supplemented with 0.8 M sorbitol, are shown.

GAL1-regulated cDNA expression library (Liu et al., 1992). From about 50,000 primary transformants selected in SC-glucose medium, a total of 12 transformants that consistently exhibited hypersensitivity to osmotin in SC-galactose medium but displayed normal sensitivity to osmotin in glucose media were selected as putative osmotin supersensitive clones. Plasmids carried by these transformants were isolated, reintroduced into BWG7a to confirm that they were able to confer galactose-dependent osmotin-supersensitive phenotype, and their cDNA inserts were sequenced. The *ORE20* gene (for *o*smotin *re*sistance), corresponding to locus *YOL002c/PHO36* (Karpichev et al., 2002), was selected for further study. This gene encodes an uncharacterized protein of 317 amino acids (36.3 kDa) that is predicted to contain seven membrane-spanning domains (*Saccharomyces* Genome Database), a characteristic feature of *G p*rotein-*c*oupled *r*eceptors (GPCRs).

The cDNA originally isolated from the screening was truncated (*PHO36t*), missing the first 19 nucleotides downstream of its hypothetical start codon. Cells of strain BWG7a overexpressing *PHO36t* from the *GAL1* promoter were more sensitive to osmotin than control cells transformed with the empty vector, and failed to form colonies in osmotin-containing media (Figure 1A).

Growth inhibition resulted from increased susceptibility to osmotin-induced cell death as demonstrated by measuring viable counts after 1 hr of osmotin treatment (data not shown). In galactose medium, the IC_{50} for osmotin of cells overexpressing *PHO36t* was 3-fold lower than that of control cells transformed with the empty vector (0.2 and 0.6 μM, respectively; data not shown). The same phenotype, in glucose medium, was observed for cells overexpressing the full-length *PHO36* from the constitutive GPD promoter in a multicopy plasmid (data not shown). Conversely, disruption of *PHO36* increased osmotin resistance (Figure 2F), which was estimated as a 3-fold increase in IC_{50} for osmotin when compared to the wild-type strain (1.6 and 0.6 μM, respectively; data not shown).

Overexpression of *PHO36* in strain BWG7a increased osmotin sensitivity of spheroplasts (Figure 1B, inset). Conversely, spheroplasts of the $\Delta pho36$ mutant were more resistant to osmotin than spheroplasts of the wild-type strain (Figure 1B). These results show that *PHO36* mediates sensitivity to osmotin at the level of the plasma membrane, unlike previously identified cell wall-mediated osmotin resistance determinants (Yun et al., 1997; Ibeas et al., 2000, 2001).

Phenotype Related to the Expression Level of *PHO36*

A $\Delta pho36$ mutant in *S. cerevisiae* strain W3031A has been reported to grow poorly on myristate and nonfermentable carbon sources (Karpichev et al., 2002). However, growth of isogenic wild-type strain BWG7a, $\Delta pho36$, and *PHO36*-overexpressing cells was indistinguishable when colony formation or cell growth rate was measured with different carbon sources (2% glucose, 2% galactose, 2% ethanol, 2% lactic acid, 2% potassium acetate, 3% glycerol, or 3% glycerol and 0.1% oleic acid; data not shown). The discrepancy perhaps results from differences in the genetic background of strains used in each study.

No differences were found in the sensitivity of wild-type, $\Delta pho36$, and *PHO36*-overexpressing cells to osmotic or ionic stresses as measured by sorbitol (2 M), NaCl, KCl, or NH_4Cl (0.75 and 1.5 M) treatments. *PHO36* was not required for invasive growth since deletion of *PHO36* in the $\Sigma 1278$ strain (Gimeno et al., 1992) did not abolish its ability to penetrate agar. The percentage of sporulation determined for diploid *PHO36/PHO36* cells (21.33 ± 5.89) and diploid $\Delta pho36/\Delta pho36$ cells (26.33 ± 3.36) were not significantly different. Subtle differences were found in mating efficiency ($\Delta pho36$, 6.9%; wild-type, 2.7%), sensitivity to heat-shock (46% ± 10% survival after 20 min at 50°C for $\Delta pho36$ cells, compared to 78.3% ± 3.38% for wild-type cells), and resistance to the cell wall perturbing agents calcofluor white and hygromycin B ($\Delta pho36$ cells were more resistant, data not shown). $\Delta pho36$ cells were previously shown to be more resistant than wild-type cells to the cell membrane perturbing antibiotic nystatin (Karpichev et al., 2002).

Expression of *PHO36* is dependent on the carbon source in the medium (Karpichev et al., 2002). Perhaps for this reason, it was difficult to predict the osmotin concentration at which the response of the $\Delta pho36$ mutant would be clearly different from that of the wild-type
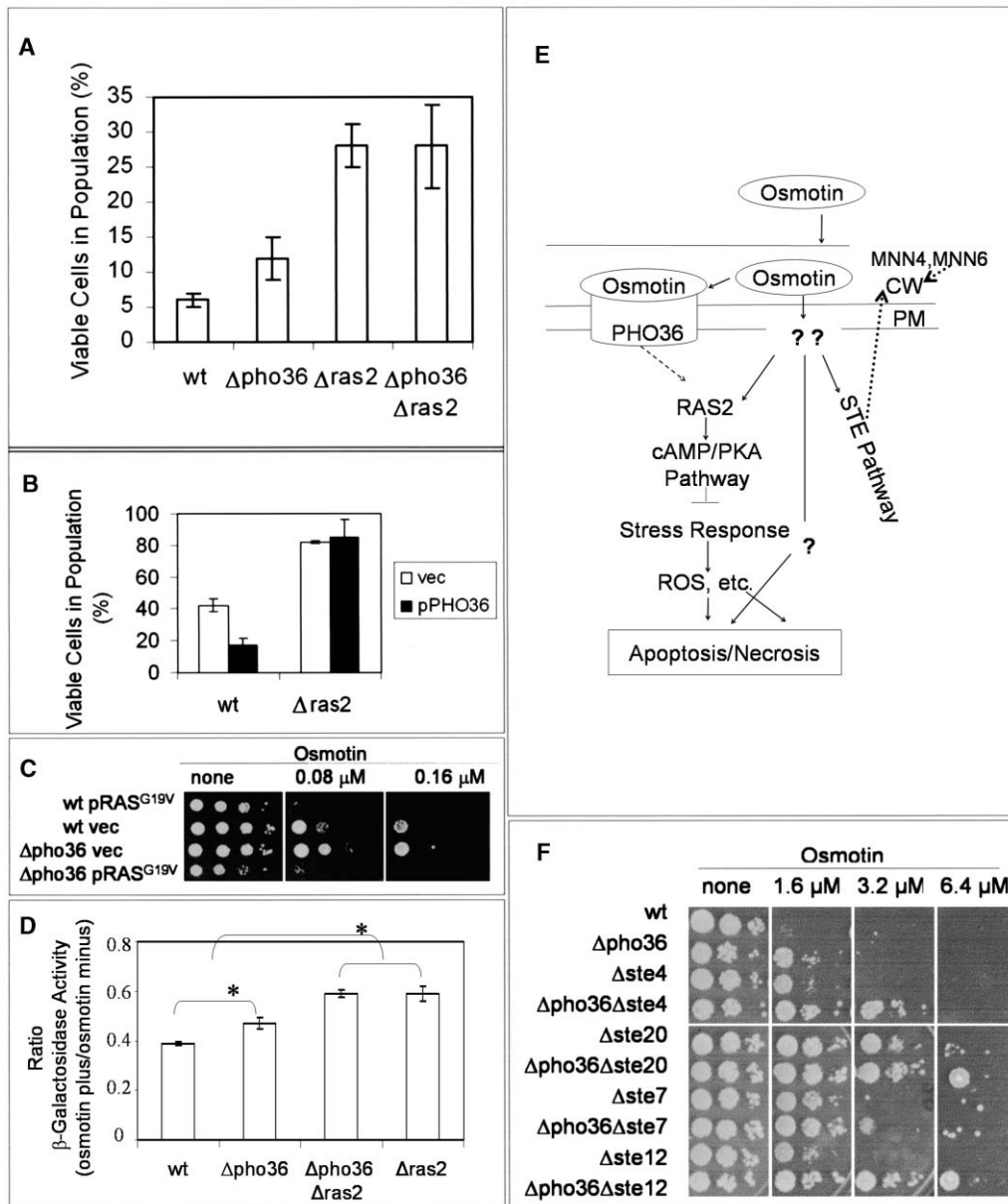
Figure 2. PHO36 Functions via *RAS2* in Osmotin-Induced Apoptosis

(A) Cells (10^8 ml^{-1}) of the wild-type strain (wt), and isogenic Δ*pho36*, Δ*ras2*, and Δ*pho36*Δ*ras2* mutant strains were incubated with 5 μM osmotin in YPD at 30°C under apoptosis-inducing conditions. Cells were washed after 3 hr osmotin treatment and the percent of total cells that were able to survive and form colonies was measured. Values represent the mean of four determinations ±SE.

(B) Cells (10^8 ml^{-1}) of wild-type (wt), and Δ*ras2* mutant strains transformed with p426GPD without (vec) or with *PHO36* insert (pPHO36) were incubated with 2 μM osmotin in selective SC-glucose medium at 30°C under apoptosis-inducing conditions. The percent of total cells able to survive and form colonies was measured after 1 hr osmotin treatment as above. Values represent the mean of two determinations ±SE.

(C) Osmotin sensitivity was assayed by spotting aliquots (2.5 μl) of serial 10-fold dilutions of A_{600nm} 0.4 cultures of strains BWG7a (wt) and Δ*pho36* mutant transformed with pAD4M (vec) or pAD4M-RAS2^{G19V} (pRAS^{G19V}) on selective SC-glucose medium without (none) or with the indicated osmotin supplements. Plates were photographed after 5 days incubation at room temperature.

(D) Cells (10^8 ml^{-1}) of strain BWG7a (wt), and isogenic Δ*pho36*, Δ*pho36*Δ*ras2*, and Δ*ras2* mutants, transformed with pSTRE-*lacZ*(*LEU2*), were treated without (minus) or with (plus) 8 μM osmotin in YPD for 45 min at 30°C under apoptosis-inducing conditions. Shown are the ratios of β-galactosidase activities measured in cell-free extracts. Each bar represents the mean ± SD (n = 3). Statistical comparison of the groups is reported: *p < 0.01; no asterisk, no difference. β-galactosidase activities in absence of osmotin were, respectively, 152 ± 4, 133 ± 3, 705 ± 23, and 139 ± 6 units. The experiment was repeated once with similar results.

(E) A model for osmotin-mediated cell death pathways is shown: Osmotin activates the RAS2/cAMP pathway and induces suppression of cellular stress responses (STRE-*lacZ* reporter) followed by accumulation of reactive oxygen species and cell death. Interaction of osmotin with PHO36 activates cell death via RAS2. There may be unidentified upstream components that stimulate the RAS2 cell death pathway in response to osmotin. Pathways controlling stress responses are even more complex, as evidenced by osmotin-independent effects on STRE-*lacZ* activity in a Δ*pho36*Δ*ras2* genetic background, and are not shown. Symbols: ?, unknown components; ↓, activation; ⊥, inhibition; →, cell wall weakening; CW, cell wall; PM, plasma membrane.

(F) Aliquots (2.5 μl) of 10-fold serial dilutions of A_{600nm} 0.4 cultures of strain BWG7a (wt) and the indicated mutant strains were spotted on YPD agar without (none) or with the indicated osmotin supplements. Plates were photographed after incubation for 2 days at 28°C.

strain. The phenotype was uncovered by comparing osmotin resistance of the wild-type and mutant strains over a few osmotin concentrations in every experiment.

PHO36 Functions in the RAS2 Signaling Pathway Activated by Osmotin to Induce Cell Death

Osmotin suppresses cellular stress signaling via the RAS2/cAMP pathway to promote programmed cell death (Narasimhan et al., 2001). Thus, osmotin resistance is increased by null mutation of *RAS2* and decreased by expression of the dominant active *RAS2*^{G19V} allele in the wild-type strain (Narasimhan et al., 2001). Mutation of *PHO36* in a Δ*ras2* mutant did not increase osmotin resistance of the Δ*ras2* mutant under apoptosis-inducing conditions (Narasimhan et al., 2001), suggesting that *PHO36* functions in the *RAS2*-mediated osmotin-induced apoptotic pathway (Figure 2A). Overexpression of *PHO36* from a multicopy plasmid in the Δ*ras2* mutant did not significantly increase osmotin sensitivity, whereas overexpression of *PHO36* in the wild-type strain rendered it more sensitive to osmotin (Figure 2B). Expression of the dominant active *RAS2*^{G19V} allele in the Δ*pho36* mutant increased sensitivity to osmotin (Figure 2C). STRE (*stress responsive*) promoter elements fused to a *lacZ* reporter gene have been shown to respond to RAS2/cAMP pathway-dependent stress signaling (Stanhill et al., 1999). The chimeric STRE-*lacZ* construct has also been used to demonstrate that osmotin suppresses cellular stress signaling via the RAS2/cAMP pathway to promote cell death (Narasimhan et al., 2001) and was used here to examine the role of *PHO36* in osmotin-induced cellular signaling (Figure 2D). Consistent with the earlier report that the extent of cell death in a population of osmotin-treated yeast cells is proportional to suppression of STRE-*lacZ* reporter gene activity (Narasimhan et al., 2001), suppression of β-galactosidase activity was greatest in wild-type cells, lower in the Δ *pho36* mutant and least in the Δ*ras2* and the Δ*pho36*Δ*ras2* double mutants (Figures 2A and 2D). These results indicate that PHO36 functions in the cell death signaling pathway upstream of RAS2. It should be noted that in the absence of osmotin treatment, STRE-*lacZ* activity in the Δ*pho36*Δ*ras2* double mutant was lower than that in the Δ*ras2* mutant (Figure 2D, legend), indicating that there are *RAS2*-independent osmotin-independent pathways controlling stress responses that become evident only in the absence of PHO36.

These and earlier data (Yun et al., 1998; Ibeas et al., 2000; Narasimhan et al., 2001) are consistent with the occurrence of yet unidentified pathways controlling osmotin toxicity (Figure 2E). For example, partial osmotin resistance of the Δ*pho36* mutant relative to that of the Δ*ras2* mutant could be explained by functional redundancy of PHO36 with other protein(s). The hypothetical protein encoded by the YDR492w locus shares the greatest identity (44%) with *PHO36*. Therefore, osmotin sensitivities of strains bearing Δ*ydr492* and Δ*pho36*-Δ*ydr492* mutations were tested but were found to be indistinguishable from those of the wild-type and Δ*pho36* strains, respectively (data not shown).

Since PHO36 has the structural features of a G protein-coupled receptor, but mediates osmotin sensitivity, the possibility that PHO36 might act as the receptor linked to the MAP kinase pathway that is activated by osmotin (Yun et al., 1998) was tested. Simultaneous disruption of *PHO36* in Δ*ste18*, Δ*ste20*, Δ*ste7*, and Δ*ste12* mutants resulted in greater osmotin resistance than disruption of either gene alone (Figure 2F), indicating that *STE* genes and *PHO36* function in different processes leading to osmotin sensitivity. This is consistent with results that place PHO36 in the RAS2 signaling pathway, since previous observations showed that *RAS2* and the *STE* genes function in genetically distinct pathways leading to osmotin sensitivity (Narasimhan et al., 2001).

Full sensitivity to osmotin requires the presence of mannosylphosphate residues on cell wall glycoproteins (Ibeas et al., 2000). Addition of mannosylphosphate is dependent on the mannosylphoshate transferase MNN6. Mutation of PHO36 increased osmotin resistance of a Δ*mnn6* mutant and overexpression of *PHO36* increased osmotin sensitivity of the Δ*mnn6* mutant as expected if they functioned in different processes regulating osmotin resistance (data not shown).

These data collectively and consistently support the conclusion that PHO36 functions upstream of RAS2 in the programmed cell death signaling pathway activated by osmotin.

PHO36 Is a Plasma Membrane Protein

PHO36 has the structural features of GPCRs. Typically these proteins are integral plasma membrane proteins. The subcellular localization of PHO36 was therefore determined using an immunocytochemical procedure for electron microscopy. For this purpose, a recombinant PHO36MH protein, in which a c-*myc* epitope and a hexa-His tag were fused in-frame at the C-terminal of PHO36, was expressed in BWG7a cells from the constitutive GPD promoter (Figure 3A). Overexpression of PHO36MH from a multicopy plasmid increased osmotin sensitivity (data not shown), indicating that PHO36MH was functional. PHO36MH was detected with myc1-9E10 monoclonal antibodies on ultrathin sections of spheroplasts generated from cells expressing low levels of PHO36MH from the single copy plasmid pPHO36MHS. Gold particle labeling indicated a plasma membrane localization of PHO36MH (Figures 3B and 3C). Accordingly, PHO36MH was immunodetected in the denser fractions of total membranes fractionated on a sucrose gradient (Figure 3D), and cofractioned with plasma membrane H$^+$-ATPase (Figure 3E), but not with vacuolar α-mannosidase (Figure 3F).

PHO36 Binds Specifically to Active PR-5 Isoforms

Membrane fractions purified from cell lysates of the PHO36MH-overexpressing strain and the Δ*pho36* mutant were incubated with osmotin-Sepharose-4B. After extensive washing, bound proteins were dissociated, separated by SDS-PAGE, and PHO36MH was immunodetected with myc1-9E10 monoclonal antibodies. Two bands representing PHO36MH monomers and dimers with apparent molecular mass of about 36 and 72 kDa, respectively, were detected in membrane fractions of the PHO36MH-overexpressing strain (Figure 4A, lanes 3–8) but were absent in membrane fractions of the Δ*pho36* mutant (Figure 4A, lane 2). No bands were detected in cell extracts of a yeast strain expressing c-*myc* tagged STE7, indicating that binding of recombinant
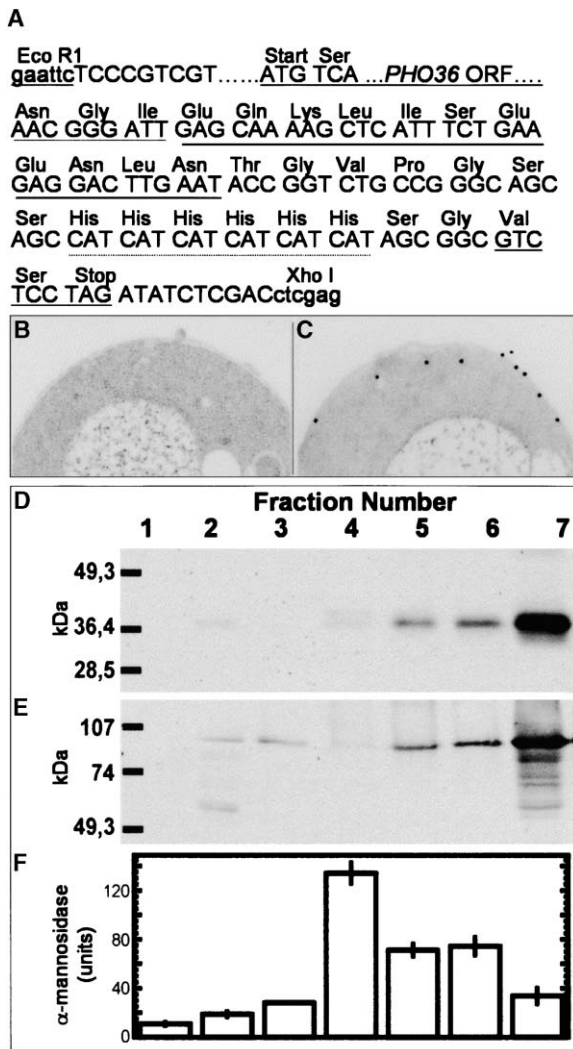
A

Eco R1   Start Ser
gaattcTCCCGTCGT......ATG TCA ...*PHO36* ORF....

Asn Gly Ile Glu Gln Lys Leu Ile Ser Glu
AAC GGG ATT GAG CAA AAG CTC ATT TCT GAA

Glu Asn Leu Asn Thr Gly Val Pro Gly Ser
GAG GAC TTG AAT ACC GGT CTG CCG GGC AGC

Ser His His His His His His Ser Gly Val
AGC CAT CAT CAT CAT CAT CAT AGC GGC GTC

Ser Stop   Xho I
TCC TAG ATATCTCGACctcgag

A

B

Figure 4. PHO36 Interacts Specifically with Osmotin In Vitro and In Vivo

(A) Osmotin-Sepharose 4B was incubated with cell extract of the strain BWG7a expressing the fusion protein STE7-Myc (lane 1), total membrane fraction purified from the strain Δ*PHO36* (lane 2) or total membrane fraction purified from the strain BWG7a expressing c-*myc* tagged PHO36 from the plasmid pPHO36MH (lanes 3–8) in the absence (lanes 1, 2, and 5) or presence of the competitor proteins A9 (100 μg, lane 3; or 10 μg, lane 7), osmotin (Osm; 100 μg, lane 4; or 10 μg, lane 6), or BSA (100 μg, lane 8). After extensive washing, bound proteins were dissociated, separated by SDS-PAGE, and the c-Myc tag was immunodetected with myc1-9E10 antibodies.

(B) Spheroplasts (10^9 ml^{-1}) derived from the Δ*pho36* mutant (Δ*pho36*) and the wild-type strain BWG7a carrying the plasmid pPHO36MH (pPHO36) were incubated with ^{35}S-osmotin (0.4 μM, 0.16 μCi) for 1 hr, without (none) or with a 10-fold molar excess of A9, BSA, or osmotin as competitors. After extensive washing, ^{35}S-osmotin retained on spheroplasts was counted.

Figure 3. PHO36 Is Localized on the Plasma Membrane

(A) The *PHO36MH* construct sequence is shown. The EcoR1-Xho1 fragment contained 46 nt of the *PHO36* gene preceding the start codon, and the natural *PHO36* ORF (thin) fused in-frame near its C terminus to a c-*myc* tag (thick) and a His tag (dotted underline).
(B–C) Immunogold localization of tagged PHO36MH protein. Ultra-thin sections of spheroplasts of strain BWG7a carrying the single copy plasmid p416GPD without (B) or with the *PHO36MH* insert (pPHO36MHS [C]) are shown. The 20 nm gold particles, which appear as small black dots, indicate the location of PHO36MH protein.
(D–F) Distribution of PHO36MH protein in cellular membranes. Extracts of cells carrying pPHO36MHS were fractionated, and distribution of proteins in the membrane-free supernatant fraction (lane 1), total membrane fraction (lane 2), and in sucrose density gradient membrane fractions, from lighter to denser fractions (lanes 3–7, respectively) was analyzed. PHO36MH (D) and plasma membrane H$^+$-ATPase marker (E) were detected on blots of proteins separated by SDS-PAGE with myc1-9E10 monoclonal antibodies and PMA1 antibodies, respectively. The activity of the vacuolar α-mannosidase marker was measured in these fractions (F) and is given in arbitrary units as increments of A$_{400nm}$ min^{-1} mg^{-1} protein.

PHO36MH to osmotin was specific for PHO36 and not the c-*myc* tag (Figure 4A, lane 1). Inclusion of free osmotin in the binding reaction reduced binding whereas inclusion of A9 or BSA had no effect (Figure 4A, lanes
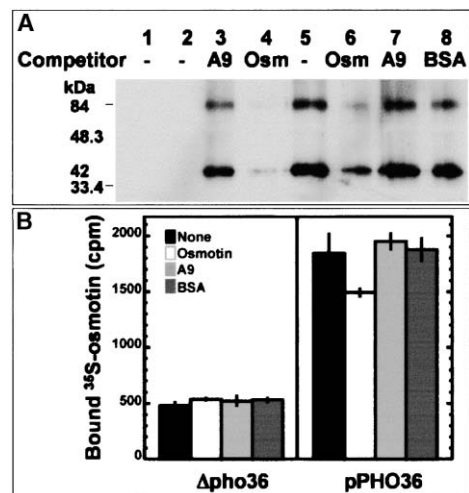
3–8), demonstrating the specificity of the osmotin-PHO36 interaction. A9, purified from the plant *Atriplex nummularia*, is a PR-5 protein that is much less active against yeast cells and spheroplasts than osmotin but is active against other fungal species (Yun et al., 1997).

Spheroplasts of the strain overexpressing *PHO36MH*, the Δ*pho36* mutant (Figure 4B), and the wild-type strain transformed with empty vector (data not shown) all bound ^{35}S-osmotin in vivo. The amount of ^{35}S-osmotin that was bound to spheroplasts of the Δ*pho36* mutant and could not be displaced by a 10-fold excess of cold osmotin during incubation represents the extent of nonspecific binding (Figure 4B, left). After subtracting this nonspecific binding, it was estimated that ^{35}S-osmotin binding to spheroplasts of the *PHO36MH*-overexpressing strain was linear for 60 min without loss of spheroplast viability (data not shown). Spheroplasts of the *PHO36MH*-overexpressing strain bound approximately three times more ^{35}S-osmotin than spheroplasts of the wild-type strain transformed with empty vector (data not shown). The binding of ^{35}S-osmotin to spheroplasts of the strain overexpressing *PHO36MH* (Figure 4B, right) was partially competed by inclusion of a 10-fold excess of cold osmotin in the reaction, but was not competed either by A9 (the inactive osmotin homolog) or BSA. Thus PHO36, the plasma membrane protein required for maximal sensitivity to osmotin, is also involved in the

specific binding of osmotin to yeast spheroplasts that precedes cell death.

Osmotin and Adiponectin Molecules Exhibit Similar Overall Structural Fold and Biological Activity

AdipoR1 and AdipoR2, the mammalian homologs of PHO36, are the receptors for adiponectin, a protein hormone secreted by adipocytes. Adiponectin deficiency in mice and humans is associated with insulin resistance and glucose intolerance (Yamauchi et al., 2001a, 2001b; Kubota et al., 2002; Diez and Iglesias, 2003). Increasing adiponectin levels by injection, overexpression, or combined weight loss and thiazolidinedione treatment protected mice and humans from diabetes, reduced insulin resistance (Yamauchi et al., 2001a, 2001b, 2003b), and reduced serum-free fatty acids, glucose, and triglycerides levels (Fruebis et al., 2001; Diez and Iglesias, 2003). Adiponectin is a 30 kDa protein with an N-terminal domain that is collagen-like and a C-terminal globular domain that is complement 1q-like (Scherer et al., 1995). The C-terminal globular domain (17 kDa) is often referred to as globular adiponectin, and Dr. Lodish and coworkers have reported that a small amount of globular adiponectin was detected in human plasma (Fruebis et al., 2001). We and others have reported that globular adiponectin has biological activities in myocytes or skeletal muscle (such as AMP kinase activation, glucose uptake, and fatty acid oxidation) as potent as full-length adiponectin (Fruebis et al., 2001; Yamauchi et al., 2001a, 2003a, 2003b). Osmotin is a globular protein (26 kDa) that has no significant sequence homology ($\leq$10%) with full-length or globular adiponectin (data not shown). X-ray crystallographic studies have shown that both globular adiponectin and osmotin consist of antiparallel β strands arranged in the shape of a β barrel (Shapiro and Scherer, 1998; Min et al., 2004). The domain I (lectin-like domain) of osmotin can be overlapped with adiponectin with a rmsd of 3.1 Å for 121 Cα atoms, suggesting that the two proteins share the lectin-like domain (Figure 5). Amino acids essential for the sweetness of thaumatin map to a cleft on its surface, which is also predicted to be important for the antifungal activity of PR-5 proteins (Figures 5A and 5B) (Kaneko and Kitabatake, 2001; Min et al., 2004). Interestingly, this region is localized on the outer surface of the adiponectin trimer. Its importance, if any, to the osmotin/PHO36 or adiponectin/adiponectin receptor interaction remains to be determined by mutational analyses. The major difference in adiponectin and osmotin structure is the presence of two extra domains in osmotin (domain II and III), which are stabilized by disulfide bonds and encompass the core lectin-like domain (domain I, Figures 5A and 5B).

Binding of adiponectin to adiponectin receptors results in activation of AMP kinase by phosphorylation (Yamauchi et al., 2003a). Adiponectin and osmotin are able to induce phosphorylation of AMP kinase in C2C12 myocytes (Figure 5C, lanes 4–8, row 1), whereas A9, the plant homolog lacking fungicidal activity against yeast, cannot (Figure 5C, lanes 9–11, row 1). Phosphorylation of AMP kinase requires expression of the adiponectin receptors AdipoR1 and AdipoR2 (Figure 5C, rows 2 and 3). Thus, the conserved biological function of adiponectin and osmotin in C2C12 myocytes must be due to a common structure in the β barrel domain (domain 1) that is involved in interaction with the adiponectin receptors.

Discussion

The Role of PHO36 in Cellular Metabolism and Osmotin-Induced Cell Death

PHO36, which encodes a plasma membrane-localized polypeptide with seven putative transmembrane domains, has the only hallmarks conserved among GPCRs. PHO36 has been inferred to have a regulatory role in lipid, phosphate, and zinc metabolism because (1) *PHO36* expression was induced by phosphate, the C$_{14:0}$ fatty acid myristate, and the oleate-dependent transcription factors OAF1 and PIP2; (2) various genes involved in fatty acid metabolism and phosphate signaling are induced in a *pho36* mutant; (3) the *pho36* mutant had high levels of acid phosphatase and accumulated polyphosphate in vacuoles; (4) the *pho36* mutant was resistant to the sterol binding antibiotic nystatin; (5) the *pho36* mutant grew poorly on glycerol plus myristate as a carbon source (Karpichev et al., 2002); and (6) *PHO36* expression is controlled by zinc levels in the growth medium and by the transcription factor ZAP1 that senses zinc deficiency (Lyons et al., 2004). It is possible that osmotin resistance is a consequence of the pleiotropy of *PHO36*. However, several facts strongly support the possibility that osmotin interacts with PHO36 affecting its natural function: (1) PHO36 interacts specifically with osmotin in solution; (2) radiolabeled osmotin binding to the plasma membrane, as well as the susceptibility to osmotin, correlates with the abundance of PHO36; and (3) adiponectin and osmotin (proteins whose main chain fold can be overlapped) participate in the same intracellular signaling pathway in C2C12 myocytes via adiponectin receptors (i.e., via mammalian homologs of PHO36). Incidentally, thaumatin, a sweet-tasting structural homolog of osmotin, binds to sweet taste receptors that are GPCRs (Li et al., 2002; http://www.cmbi.kun.nl/7tm/). Hence, the ability to bind to GPCRs could be a conserved characteristic of PR-5 proteins (Veronese et al., 2003) that contributes to their specificity for a subset of fungal species targets.

The evidence that *PHO36* and *RAS2* function in the same pathway is consistent with a role for *PHO36* in nutrition sensing. RAS proteins in yeast are linked to cell division, differentiation, apoptosis, longevity, carbon, and nitrogen nutrition (Jazwinski, 1999; Narasimhan et al., 2001; Forsberg and Ljungdahl, 2001). Adiponectin receptors regulate glucose uptake, fatty acid β-oxidation, and the activities of some proteins that sense the energy status of the cell (Yamauchi et al., 2003a). Because of the link with apoptosis, it would be worthwhile to investigate if PHO36 is connected to the regulation of nutrient acquisition and metabolism in response to cellular energy status or mitochondrial (dys)-function. Recent reports show that adiponectin induces apoptosis in epithelial cells (Bråkenheilm et al., 2004).

Unlike typical GPCRs, the adiponectin receptors are not coupled with G proteins, although they do activate distinct signaling molecules (Yamauchi et al., 2003a). We found no evidence for the involvement of the yeast Gα subunits GPA1 or GPA2 in osmotin-induced cell death (data not shown). STE4 and STE18 (Gβ and Gγ subunits) are also not coupled to PHO36 (Figure 2F). Therefore PHO36 may either not be coupled to heterotrimeric G-proteins like the adiponectin receptors (Yamauchi et al., 2003a) or may be coupled to the unusual
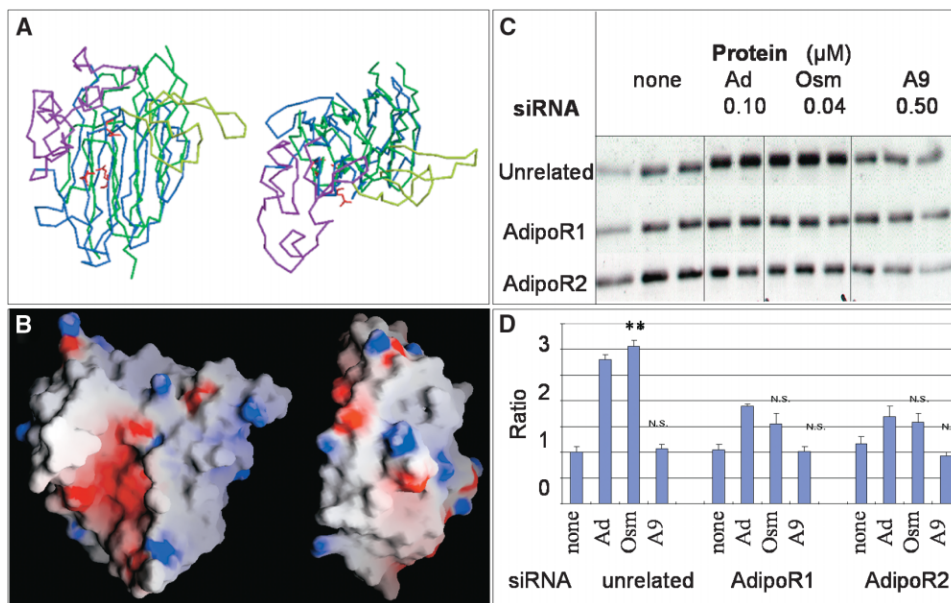
Figure 5. Comparison of the Structures of Osmotin and Adiponectin

(A) Shown are monodiagrams with two different views (90° rotation) of the superposition of the Cα traces of osmotin (yellow-green, blue, and magenta) and adiponectin (green). Three domains of osmotin are colored blue (domain I or lectin-like domain), magenta (domain II, amino acids 121–177), and yellow-green (domain III, amino acids 55–82). Three conserved residues which are found in the acidic cleft of osmotin family (Glu84, Asp97, and Asp102) are drawn in red stick models.

(B) View of the surface topology of osmotin (left) and adiponectin (right) showing the surface electrostatic potential. Protein surface is colored according to the electrostatic potential from blue (most positive) to white (neutral) to red (most negative). The protein orientations are identical to those shown in (A) (left). The figure was drawn using GRASP (Nicholls et al., 1991).

(C) Shown are immunoblots of lysates (10 μg protein per lane) of C2C12 myocytes transfected with the indicated siRNAs and treated without (none) or with the indicated concentrations of full-length adiponectin (Ad), osmotin (Osm), and A9 (A9) for 10 min and probed with phosphoAMP kinase-specific antibodies.

(D) Quantitative analyses of the data in (C). Statistically significant (**) and insignificant (N.S.) difference compared to values with no added protein (none) in the same siRNA set are indicated.

proteins associated with GPA2 (Harashima and Heitman, 2002).

Genetic evidence places *PHO36* function upstream of *RAS2* in the osmotin-induced apoptotic pathway (Figure 2), consistent with its plasma membrane location (Figure 3). Since the effect of PHO36 on osmotin sensitivity is smaller than the effect of RAS2, our data raise the possibility that other "receptors" also connect to the RAS2 pathway.

Pharmacological Significance of the Similarity between Osmotin and Adiponectin Molecules

The homology shared by their plasma membrane "receptors" indicates that similar "receptor binding sites" exist on osmotin and adiponectin. In fact, osmotin is able to induce adiponectin receptor-mediated AMP kinase phosphorylation in C2C12 myocytes (Figure 5C). This evidence underlines two extraordinary facts. First, two proteins with no sequence identity and a structural fold that is fairly common among several proteins (Jones et al., 1989; Eck and Sprang, 1989; Karpusas et al., 1995; Shapiro and Scherer, 1998) share a highly specific functional activity that has major significance in human disease. Second, osmotin is a member of a large PR-5 protein family (24 members in *Arabidopsis thaliana*) that is both ubiquitous (all plant species screened have been reported to contain PR-5 proteins) and diverse (almost all of the PR-5 protein genes sequenced from many

different species are only about 50% identical [Veronese et al., 2003]). PR-5 proteins are also extremely stable and may remain active when in contact with human digestive or respiratory systems, as some are known to be significant allergens (Breiteneder and Ebner, 2000). Therefore, their functional similarity to adiponectin raises important questions about their possible role in human and animal health, considering their abundance in plant tissues (seeds, fruits, pollen). Most important is our finding that a homologous activity (AMP kinase activation) is shared by osmotin and adiponectin and is mediated through mammalian adiponectin receptor. This strongly suggests that further research examining similarities in adiponectin and osmotin function may facilitate efficient screening of potential adiponectin receptor agonists (chemical, natural-occurring, and mutation-generated variants of PR-5 proteins) by PHO36-mediated phenotype analyses in *S. cerevisiae*.

Experimental Procedures

Strains, Plasmids, and Media

Escherichia coli DH5α was used for plasmid propagation and isolation. All the *Saccharomyces cerevisiae* strains were isogenic derivates of BWG7a (Becker and Guarante, 1991). Strain BWG7α was obtained by mating type switching with the *HO* gene (Herskowitz and Jensen, 1991). The Δste, Δras2, and Δmnn6 mutants and procedures for disruption of these loci have been described elsewhere (Yun et al., 1998; Narasimhan et al., 2001). The *PHO36* locus was

deleted by replacing an internal coding sequence with *URA3* (+192 to +680 bp relative to the second ATG that is predicted to be the start codon) or *kanMX* (+72 to +740 bp) as described (Wach et al., 1997). The Δ*ydr492* mutation was created by replacing an internal coding sequence (+244 to +724 bp) with *LEU2*. Precise gene disruptions were confirmed by PCR and Southern blotting. The diploid Δ*pho36*/Δ*pho36* mutant strain was made by crossing the opposite mating type haploid strains.

For constitutive overexpression, pPHO36 was constructed by isolating the coding region of PHO36 (−46 to +957 bp) from strain BWG7a by PCR and by cloning it into the multicopy plasmid p426GPD (Mumberg et al., 1995). The plasmid pPHO36MH was constructed from pPHO36 by introducing c-*myc* and hexa-His tags in-frame at the C terminus of PHO36 by PCR. Construct PHO36MH was sequenced to confirm proper fusion of tags. For low-level expression of tagged PHO36, the plasmid pPHO36MHS was made by cloning the PHO36MH construct in the single copy plasmid p416GPD using appropriate restriction enzyme sites. The plasmid pNC267 containing STE7-Myc translational fusion has been described (Zhou et al., 1993). RAS2^{G19V} was cloned in pAD4M. To construct STRE-*lacZ* (*LEU2*), the chimeric STRE-*lacZ* gene from pSTRE-*lacZ*(*TRP*) (Stanhill et al., 1999) was isolated by PCR using 5′-CCC AAGCTTCAGTTATTACCCTCGAC-3′ as forward primer and 5′-CCC GGGTTATTTTTGACACCAGACCAA-3′ as reverse primer. The insert was subcloned into pGEM-T easy, sequenced, excised with ApaII and XmaI, and subcloned into the corresponding sites of pRS315.

Standard procedures were used for yeast media preparation and genetic analyses (Becker and Guarante, 1991; Sherman, 1991). Yeast transformations were performed by the lithium acetate method (Elble, 1992). Analysis of yeast strain phenotype was performed according to standard procedures (Hampsey, 1997).

cDNA Library and Cloning

Strain BWG7a was transformed with a *GAL1*-regulated yeast cDNA expression library (Liu et al., 1992). Approximately 50,000 primary transformants selected on SC-glucose medium were replica-plated sequentially onto 0.003% methylene blue containing selective SC-galactose medium without or with osmotin (0.2 μM), a sublethal concentration under these conditions. Transformants that turned blue or failed to grow in presence of osmotin were then selected. The galactose-dependent osmotin supersensitive phenotype of these transformants was confirmed by spot assays on selective SC-galactose and SC-glucose media with a range of osmotin supplements. Plasmids carried by these transformants were isolated (Robzyk and Kassir, 1992) and their cDNA inserts were sequenced.

Purification of Total Membranes and Subcellular Fractionation

Total membrane fraction was isolated from 1 liter cultures (A$_{600nm}$ 1.0) of yeast cells expressing PHO36MH from the single copy plasmid pPHO36MHS as described (David et al., 1997). It was resuspended in 3 ml of 10% (w/w) sucrose in buffer A (50 mM HEPES, [pH 7.5], 5 mM EDTA, 2 μg ml^{-1} aprotinin, 2 μg ml^{-1} chymostatin, 2 μg ml^{-1} pepstatin, 1 μg ml^{-1} leupeptin, 2 mM benzamidine, 1 mM PMSF) and layered on top of a five step sucrose gradient (15, 28, 35, 43, and 53% w/w) in buffer A (2 ml per step). After centrifugation for 12 hr at 20,000 rpm in a Beckman SW40 rotor at 4°C, fractions (2 ml) were collected from top to bottom. They were diluted with three volumes of water and centrifuged at 186,000 × g for 30 min. The pellets were resuspended in 200 μl of buffer (10 mM Mes.KOH, [pH 6.5], 10% glycerol, protease inhibitors as in buffer A).

Protein Methods and Enzyme Assays

Osmotin purification and assays of osmotin cytotoxicity were performed as described previously (Yun et al., 1997; Ibeas et al., 2000; Narasimhan et al., 2001). α-Mannosidase activity was measured using p-nitrophenyl-α-D-mannopyranoside (Sigma) as substrate. Protein concentration was determined with the Bio-Rad protein assay kit (Bio-Rad). Protein extracts were fractionated by SDS-PAGE on 10% polyacrylamide gels and transferred to nitrocellulose membranes. PHO36MH and the plasma membrane H$^+$-ATPase were detected on immunoblots of the separated proteins by the ECL method (Amersham Biosciences). Myc1-9E10 monoclonal antibodies (2 μg ml^{-1}; CalBiochem) and rabbit PMA1 polyclonal antibodies

(1:10000 dilution) (Monk et al., 1991) were used as primary antibodies, and horseradish peroxidase-conjugated anti-mouse or anti-rabbit immunoglobulin G (1:5000 dilution; Promega) were used as secondary antibodies. β-Galactosidase assay method, cell growth conditions, osmotin treatments, and preparation of cell extracts for this purpose have been described earlier (Narasimhan et al., 2001). β-galactosidase activities were expressed in arbitrary units as increments of A$_{400nm}$ min^{-1} mg^{-1} protein. The protocols for purifying recombinant murine adiponectin and measuring activation of AMP kinase in murine C2C12 myocytes have been described (Yamauchi et al., 2003a).

Immunogold Localization

Yeast spheroplasts were fixed and embedded as described (Yun et al., 1997) except that 1 M sorbitol was added to the fixative solution as osmotic stabilizer and that sodium metaperiodate treatment was omitted. Ultrathin sections were reacted successively with myc1-9E10 monoclonal antibodies (5 μg ml^{-1}) and goat anti-mouse IgG conjugated to 20 nm gold particles (1:50 dilution; Ted Pella, Inc.; Redding, CA). Sections were viewed with a transmission electron microscope EM200 (Philips Electronic Instruments Co., Mahwah, NJ).

^{35}S-Osmotin Binding Assay

Osmotin was radiolabeled to a specific activity of 12 Ci mmol^{-1} using the ^{35}SLR reagent (Amersham), according to manufacturer's instructions. Yeast cells were grown in YPD medium until A$_{600nm}$ 0.6 and then harvested by centrifugation. The pellet was resuspended in 1 M sorbitol (to A$_{600nm}$ 6) and treated with lyticase (100 U ml^{-1}). After digestion of the cell wall was completed, spheroplasts were collected by centrifugation, washed twice with 1 M sorbitol, and resuspended in 1 M sorbitol (10^9 ml^{-1}). The binding reaction was initiated by the addition of 2 μl of ^{35}S-osmotin (1 μCi, 3 μg) to 300 μl of spheroplasts (0.3 × 10^9). After 60 min incubation at 30°C, triplicate aliquots (50 μl) of the reaction mixture were diluted into ice-cold 1 M sorbitol (1.5 ml). Spheroplasts were collected by centrifugation, washed twice, resuspended in 1 M sorbitol (50 μl) and counted in a liquid scintillation counter in 5 ml of EcoLume (ICN Biomedicals). For competition experiments, spheroplasts were preincubated for 30 min with A9, osmotin, or BSA before adding ^{35}S-osmotin.

Protein Interaction Assays in Solution

Osmotin was coupled to CNBr-activated Sepharose 4B (Pharmacia Biotech) according to the manufacturer's instructions. Total membrane fraction (from 50 ml culture) was isolated as described earlier and resuspended in 200 μl of buffer (1% n-dodecyl-β-D-maltoside, 10% glycerol, 50 mM Tris.HCl [pH 7.6], 100 mM NaCl, 1 mM PMSF). Total membrane fraction (50 μl) was incubated with osmotin-Sepharose 4B (200 μl) in 50 mM Tris.HCl (pH 7.6), 1 mM PMSF (1 ml) in the absence or presence of competitor protein (100 μg) with gentle agitation for 4 hr at room temperature. After five washes with 50 mM Tris.HCl (pH 7.6), 0.1% Triton X-100, the complexes were dissociated by incubating in sample buffer (1% SDS, 50 mM Tris.HCl [pH7.6], 10% glycerol) for 30 min at room temperature and separated by 10% SDS-PAGE. PHO36MH protein was immunodetected on blots using myc1-9E10 monoclonal antibodies.

References

Becker, D.M., and Guarante, L. (1991). High-efficiency transformation of yeast by electroporation. In Methods in Enzymology, Volume 194, C. Guthrie and G.R. Fink, eds. (New York: Academic Press), pp. 182–187.

Bråkenhielm, E., Vietnmaki, N., Cao, R., Kihara, S., Matsuzawa, Y., Zhivotovsky, B., Funahashi, T., and Cao, Y. (2004). Adiponectin-induced antiangiogenesis and antitumor activity involve caspase-mediated endothelial cell apoptosis. Proc. Natl. Acad. Sci. USA 101, 2476–2481.

Breiteneder, H., and Ebner, C. (2000). Molecular and biochemical classification of plant-derived food allergens. J. Allergy Clin. Immunol. 106, 27–36.

David, N.E., Gee, M., Andersen, B., Naider, F., Thorner, J., and Stevens, R.C. (1997). Expression and purification of the Saccharomyces cerevisiae alpha-factor receptor (Ste2p), a 7-transmembrane-segment G protein-coupled receptor. J. Biol. Chem. 272, 15553–15561.

Diez, J.J., and Iglesias, P. (2003). The role of the novel adipocyte-derived hormone adiponectin in human disease. Eur. J. Endocrinol. 148, 293–300.

Eck, M.E., and Sprang, S.R. (1989). The structure of tumor necrosis factor-α at 2.6 Å resolution. J. Biol. Chem. 264, 17595–17605.

Elble, R. (1992). A simple and efficient procedure for transformation of yeasts. Biotechniques 13, 18–20.

Forsberg, H., and Ljungdahl, P.O. (2001). Sensors of extracellular nutrients in Saccharomyces cerevisiae. Curr. Genet. 40, 91–109.

Fruebis, J., Tsao, T.S., Javorschi, S., Ebbets-Reed, D., Erickson, M.R., Yen, F.T., Bihain, B.E., and Lodish, H.F. (2001). Proteolytic cleavage product of 30-kDa adipocyte complement-related protein increases fatty acid oxidation in muscle and causes weight loss in mice. Proc. Natl. Acad. Sci. USA 98, 2005–2010.

Gimeno, C.J., Ljungdahl, P.O., Styles, C.A., and Fink, G.R. (1992). Unipolar cell divisions in the yeast Saccharomyces cerevisiae lead to filamentous growth: regulation by starvation and RAS. Cell 68, 1077–1090.

Hampsey, M. (1997). A review of phenotypes in Saccharomyces cerevisiae. Yeast 13, 1099–1133.

Harashima, T., and Heitman, J. (2002). The Galpha protein Gpa2 controls yeast differentiation by interacting with kelch repeat proteins that mimic Gbeta subunits. Mol. Cell 10, 163–173.

Herskowitz, I., and Jensen, R.E. (1991). Putting the HO gene to work: practical uses for mating-type switching. In Methods in Enzymology, Volume 194, C. Guthrie and G.R. Fink, eds. (New York: Academic Press), pp. 132–145.

Ibeas, J.I., Lee, H., Damsz, B., Prasad, D.T., Pardo, J.M., Hasegawa, P.M., Bressan, R.A., and Narasimhan, M.L. (2000). Fungal cell wall phosphomannans facilitate the toxic activity of a plant PR-5 protein. Plant J. 23, 375–383.

Ibeas, J.I., Yun, D.-J., Damsz, B., Narasimhan, M.L., Uesono, Y., Ribas, J.C., Lee, H., Hasegawa, P.M., Bressan, R.A., and Pardo, J.M. (2001). Resistance to the plant PR-5 protein osmotin in the model fungus Saccharomyces cerevisiae is mediated by the regulatory effects of SSD1 on cell wall composition. Plant J. 25, 271–280.

Jazwinski, S.M. (1999). The RAS genes: a homeostatic device in Saccharomyces cerevisiae longevity. Neurobiol. Aging 20, 471–478.

Jones, E.Y., Stuart, D.I., and Walker, N.P. (1989). Structure of tumour necrosis factor. Nature 338, 225–228.

Kaneko, R., and Kitabatake, N. (2001). Structure-sweetness relationship in thaumatin: importance of lysine residues. Chem. Senses 26, 167–177.

Karpichev, I.V., Cornivelli, L., and Small, G.M. (2002). Multiple regulatory roles of a novel Saccharomyces cerevisiae protein, encoded by YOL002c, in lipid and phosphate metabolism. J. Biol. Chem. 277, 19609–19617.

Karpusas, M., Hsu, Y.M., Wang, J.H., Thompson, J., Lederman, S., Chess, L., and Thomas, D. (1995). A crystal structure of an extracellular fragment of human CD40 ligand. Structure 3, 1031–1039.

Kubota, N., Terauchi, Y., Yamauchi, T., Kubota, T., Moroi, M., Matsui, J., Eto, K., Yamashita, T., Kamon, J., Satoh, H., et al. (2002). Disruption of adiponectin causes insulin resistance and neointimal formation. J. Biol. Chem. 277, 25863–25866.

Li, X., Staszewski, L., Xu, H., Durick, K., Zoller, M., and Adler, E. (2002). Human receptors for sweet and umami taste. Proc. Natl. Acad. Sci. USA 99, 4692–4696.

Liu, H., Krizek, J., and Bretscher, A. (1992). Construction of a GAL1-regulated yeast cDNA expression library and its application to the identification of genes whose overexpression causes lethality in yeast. Genetics 132, 665–673.

Lyons, T.J., Villa, N.Y., Regalla, L.M., Kupchak, B.R., Vagstad, A., and Eide, D.J. (2004). Metalloregulation of yeast membrane steroid receptor homologs. Proc. Natl. Acad. Sci. USA 101, 5506–5511.

Min, K., Ha, S.C., Hasegawa, P.M., Bressan, R.A., Yun, D.J., and Kim, K.K. (2004). Crystal structure of osmotin, a plant antifungal protein. Proteins 54, 170–174.

Monk, B.C., Montesinos, C., Ferguson, C., Leonard, K., and Serrano, R. (1991). Immunological approaches to the transmembrane topology and conformational changes of the carboxyl-terminal regulatory domain of yeast plasma membrane H⁺-ATPase. J. Biol. Chem. 266, 18097–18103.

Mumberg, D., Muller, R., and Funk, M. (1995). Yeast vectors for the controlled expression of heterologous proteins in different genetic backgrounds. Gene 156, 119–122.

Narasimhan, M.L., Damsz, B., Coca, M.A., Ibeas, J.I., Yun, D.-J., Pardo, J.M., Hasegawa, P.M., and Bressan, R.A. (2001). A plant defense protein induces microbial apoptosis. Mol. Cell 8, 921–930.

Narasimhan, M.L., Lee, H., Damsz, B., Singh, N.K., Ibeas, J.L., Matsumoto, T.K., Woloshuk, C.P., and Bressan, R.A. (2003). Overexpression of a cell wall glycoprotein in Fusarium oxysporum increases virulence and resistance to a plant PR-5 protein. Plant J. 36, 390–400.

Nicholls, A., Sharp, K.A., and Honig, B. (1991). Protein folding and association: insights from the interfacial and thermodynamic properties of hydrocarbons. Proteins 11, 281–296.

Robzyk, K., and Kassir, Y. (1992). A simple and highly efficient procedure for rescuing autonomous plasmids from yeast. Nucleic Acids Res. 20, 3790.

Scherer, P.E., Williams, S., Fogliano, M., Baldini, G., and Lodish, H.F. (1995). A novel serum protein similar to C1q, produced exclusively in adipocytes. J. Biol. Chem. 270, 26746–26749.

Shapiro, L., and Scherer, P.E. (1998). The crystal structure of a complement-1q family protein suggests an evolutionary link to tumor necrosis factor. Curr. Biol. 8, 335–338.

Sherman, F. (1991). Getting started with yeast. In Methods in Enzymology, Volume 194, C. Guthrie and G.R. Fink, eds. (Academic Press, New York), pp. 3–21.

Stanhill, A., Schick, N., and Engelberg, D. (1999). The yeast Ras/cyclic AMP pathway induces invasive growth by suppressing the cellular stress response. Mol. Cell. Biol. 19, 7529–7538.

Veronese, P., Ruiz, M., Coca, M.A., Hernandez-Lopez, A., Lee, H., Ibeas, J.I., Damsz, B., Pardo, J.M., Hasegawa, P.M., Bressan, R.A., et al. (2003). In defense against pathogens. Both plant sentinels and foot soldiers need to know the enemy. Plant Physiol. 131, 1580–1590.

Wach, A., Brachat, A., Alberti-Segui, C., Rebischung, C., and Philippsen, P. (1997). Heterologous HIS3 marker and GFP reporter modules for PCR-targeting in Saccharomyces cerevisiae. Yeast 13, 1065–1075.

Yamauchi, T., Kamon, J., Waki, H., Terauchi, Y., Kubota, N., Hara, K., Mori, Y., Ide, T., Murakami, K., Tsuboyama-Kasaoka, N., et al.

(2001a). The fat-derived hormone adiponectin reverses insulin resistance associated with both lipoatrophy and obesity. Nat. Med. *7*, 941–946.

Yamauchi, T., Waki, H., Kamon, J., Murakami, K., Motojima, K., Komeda, K., Miki, H., Kubota, N., Terauchi, Y., Tsuchida, A., et al. (2001b). Inhibition of RXR and PPARgamma ameliorates diet-induced obesity and type 2 diabetes. J. Clin. Invest. *108*, 1001–1013.

Yamauchi, T., Kamon, J., Ito, Y., Tsuchida, A., Yokomizo, T., Kita, S., Sugiyama, T., Miyagishi, M., Hara, K., Tsunoda, M., et al. (2003a). Cloning of adiponectin receptors that mediate antidiabetic metabolic effects. Nature *423*, 762–769.

Yamauchi, T., Kamon, J., Waki, H., Imai, Y., Shimozawa, N., Hioki, K., Uchida, S., Ito, Y., Takakuwa, K., Matsui, J., et al. (2003b). Globular adiponectin protected ob/ob mice from diabetes and ApoE-deficient mice from atherosclerosis. J. Biol. Chem. *278*, 2461–2468.

Yun, D-J., Zhao, Y., Pardo, J.M., Narasimhan, M.L., Damsz, B., Lee, H., Abad, L.R., Paino D'Urzo, M., Hasegawa, P.M., and Bressan, R.A. (1997). Stress proteins on the yeast cell surface determine resistance to osmotin, a plant antifungal protein. Proc. Natl. Acad. Sci. USA. *94*, 7082–7087.

Yun, D.-J., Ibeas, J.I., Lee, H., Coca, M.A., Narasimhan, M.L., Uesono, Y., Hasegawa, P.M., Pardo, J.M., and Bressan, R.A. (1998). Osmotin, a plant antifungal protein, subverts signal transduction to enhance fungal cell susceptibility. Mol. Cell *1*, 807–817.

Zhou, Z., Gartner, A., Cade, R., Ammerer, G., and Errede, B. (1993). Pheromone-induced signal transduction in *Saccharomyces cerevisiae* requires the sequential function of three protein kinases. Mol. Cell. Biol. *13*, 2069–2080.